Supporting Information

Aluminum doping-induced α/γ-MnO_2 heterophase and oxygen vacancy defect engineering for high-performance aqueous zinc-manganese batteries

Shiyan Wang[a, 1], Jie Feng [a, 1], Chengzu Li[a], Yulong Zhu [b], Haizou Yu[a], Panpan Sun[a, c], Xiaowei Lv[a, c], Xiaohua Sun[a, c*]

[a] College of Materials and Chemical Engineering, College of Mechanical and Power Engineering, Key Laboratory of Inorganic Nonmetallic Crystalline and Energy Conversion Materials, China Three Gorges University, Yichang, 443002, China.

[b] Hangzhou Special Equipment Inspection & Science Research Institute, Hangzhou, Zhejiang 310051, China

[c] Hubei Three Gorges Laboratory, Yichang, Hubei 443007, China

* Corresponding author. Tel.: +86-717-6397509; fax: +86-717-6397559.

E-mail address: mksxh@163.com (X.H. Sun).

1 Jie Feng and Shiyan Wang contributed equally to this work.

Supplementary Figures and Tables

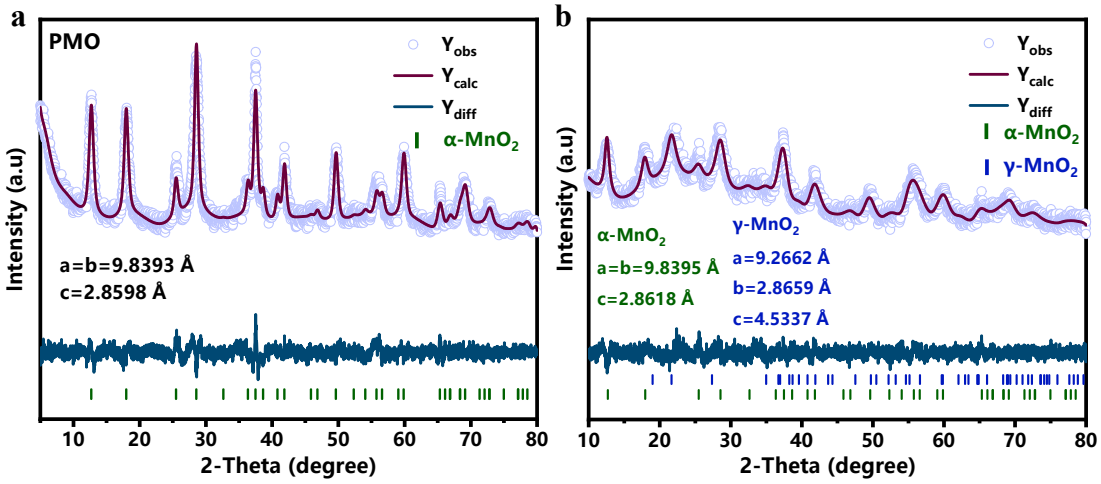

Figure S1. Rietveld refinement of (a)PMO and (b)PAMO.

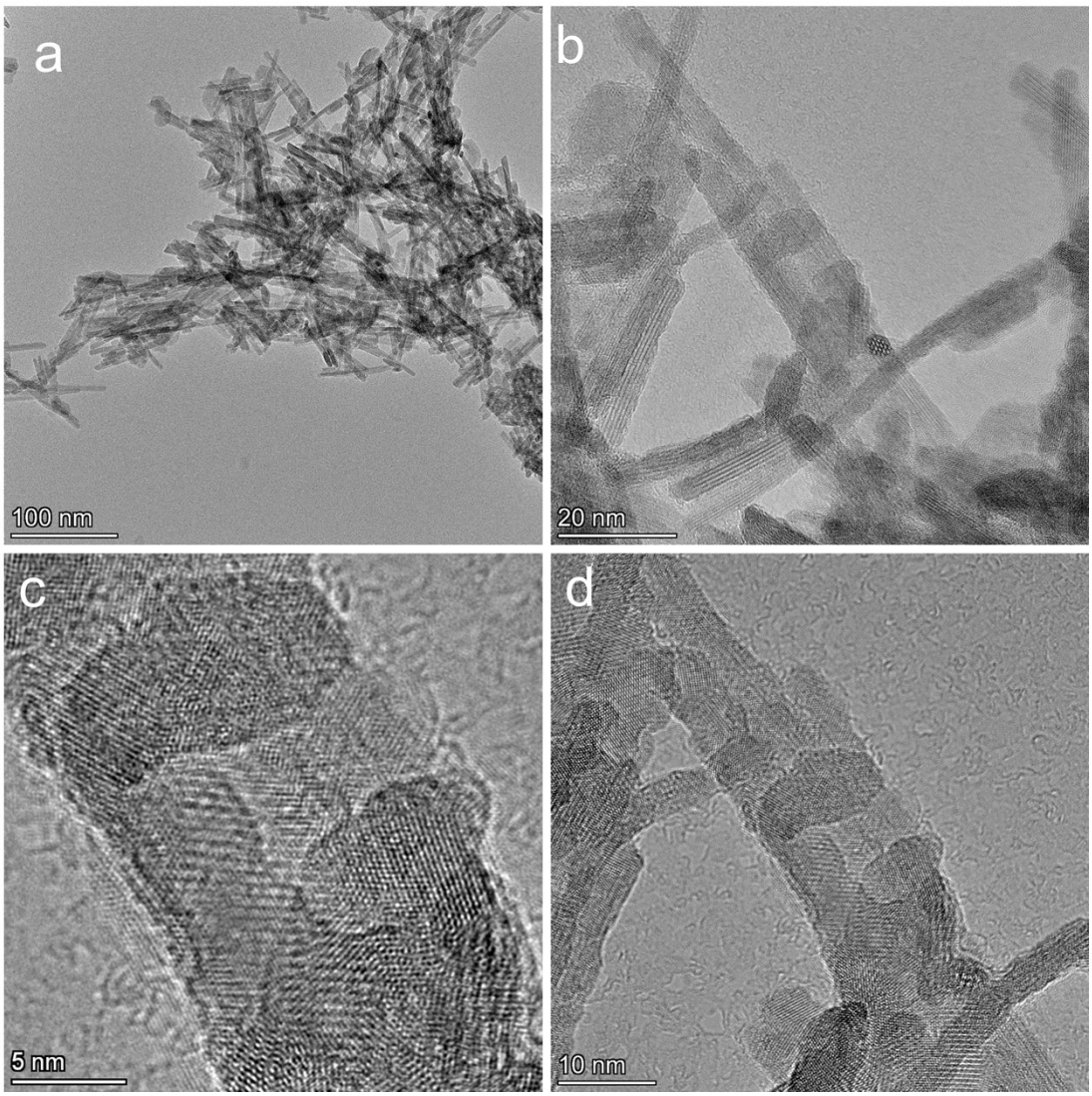

Figure S2. (a)TEM image of PAMO; (b-d) HRTEM image of PAMO.

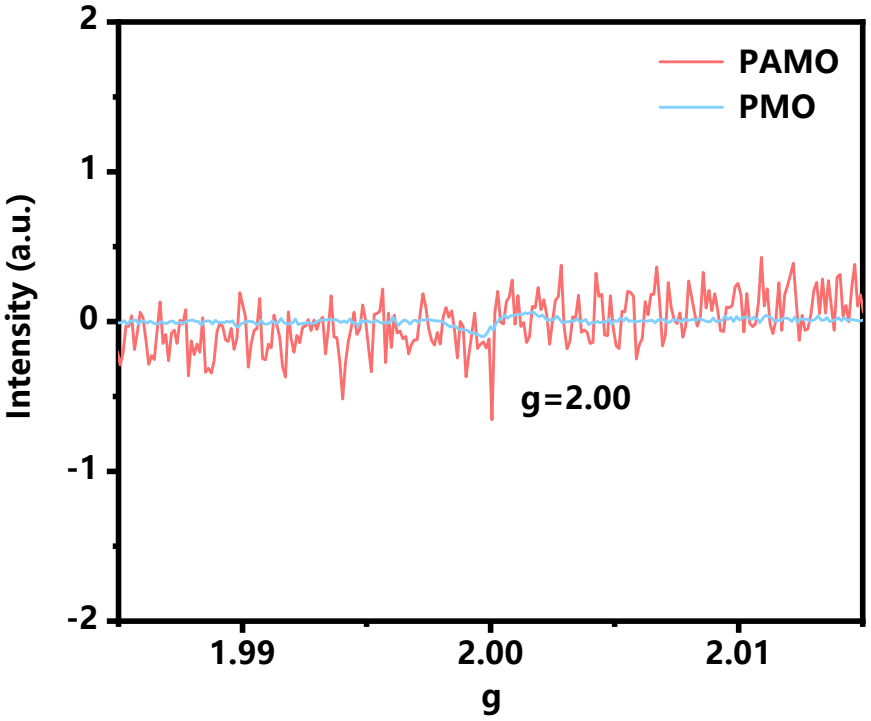

Figure S3. (a) EPR spectra of PAMO and PMO at 88K.

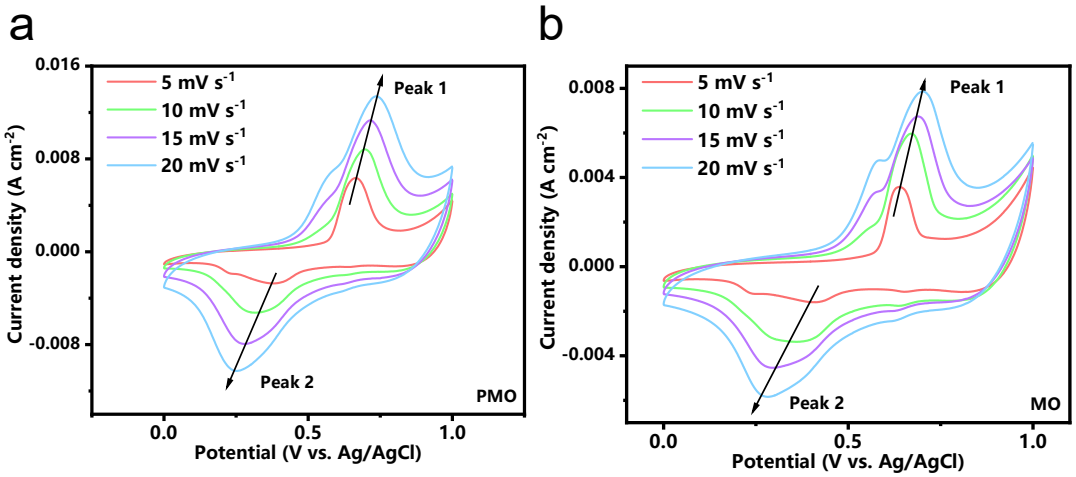

Figure S4. CV curves at different scan rates of (a) PMO and (b) MO electrodes.

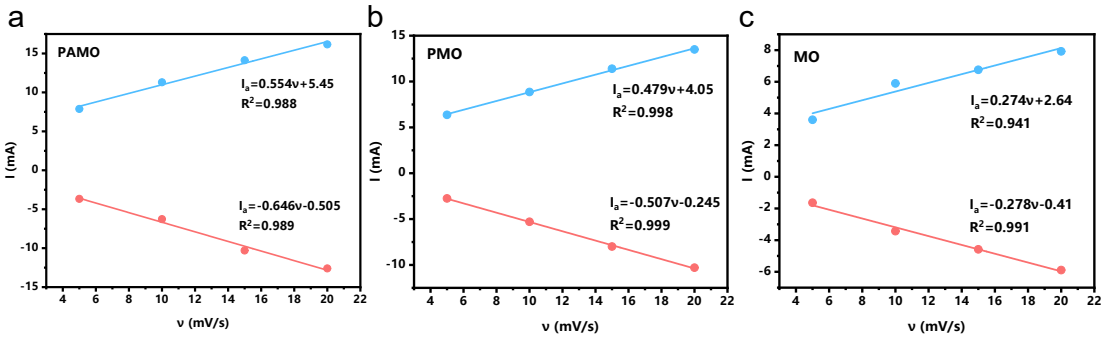

Figure S5. Surface coverage of redox species (Γ*) for (a) PAMO, (b) PMO, (c) MO electrodes.

The current densities of both the anodic and cathodic peaks demonstrate a linear increase with elevated scan rates, indicating that the redox process is predominantly governed by surface phenomena. To further quantify the density of electrochemically active sites on the electrode surface, we employed Laviron's theory for surface-controlled processes. By fitting the average slope (k) derived from the plot of peak current density (I_p) versus scan rate (ν), we estimated the surface coverage (Γ∗) of the redox species.

For electrochemical processes with purely surface control, the relationship between peak current and scan rate can be described by the following equation:

$$I_P = (n^2F^2/4RT)A\Gamma^*v \qquad \text{(S1)}$$

Wherein, **n** represents the number of electrons transferred (in this work, n = 1), **F** is the Faraday constant (96485 C mol^{-1}), **R** is the gas constant (8.314 J mol^{-1} K^{-1}), **T** is the thermodynamic temperature (298.15 K), and **A** is the geometric area of the electrode (1 cm^2).

Substituting the aforementioned constants and simplifying, we derive a reduced relationship between the surface coverage Γ* and the fitting slope k (I_p/ν):

$$\Gamma^* = 1.07 \bullet 10^{-6} \bullet k \qquad \text{(S2)}$$

Among these, the unit of Γ* is mol cm^{-2}, and the unit of k is A s V^{-1} (or C V^{-1}).

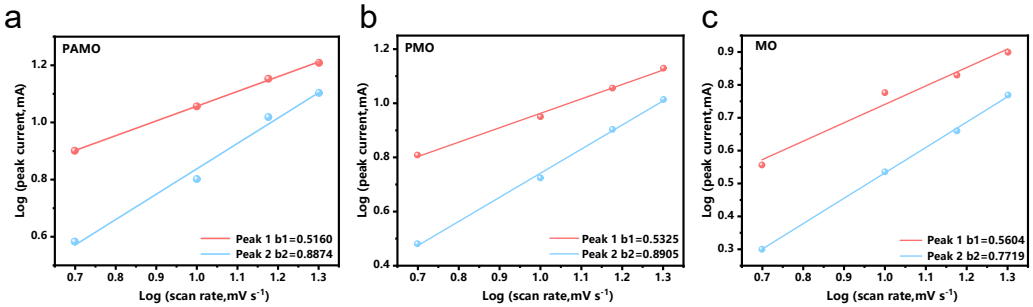

Figure S6. Plots of log (i) vs. log (v) for (a) PAMO, (b) PMO, and (c) MO electrodes to determine the b-value.

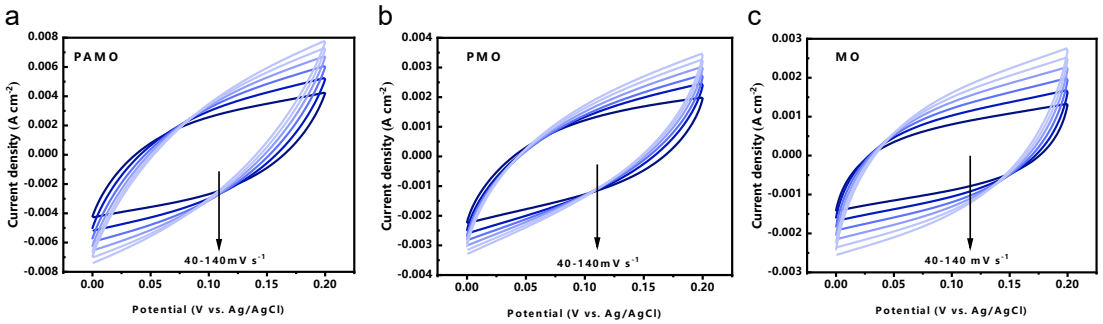

Figure S7. CV curves of the a) PAMO, b) PMO and c) MO electrodes under different scan rates in the potential window of 0 V to 0.2 V (vs. Ag/AgCl). These curves were used to present the plots showing the extraction of the C_{dl} for different samples shown in the Figure.

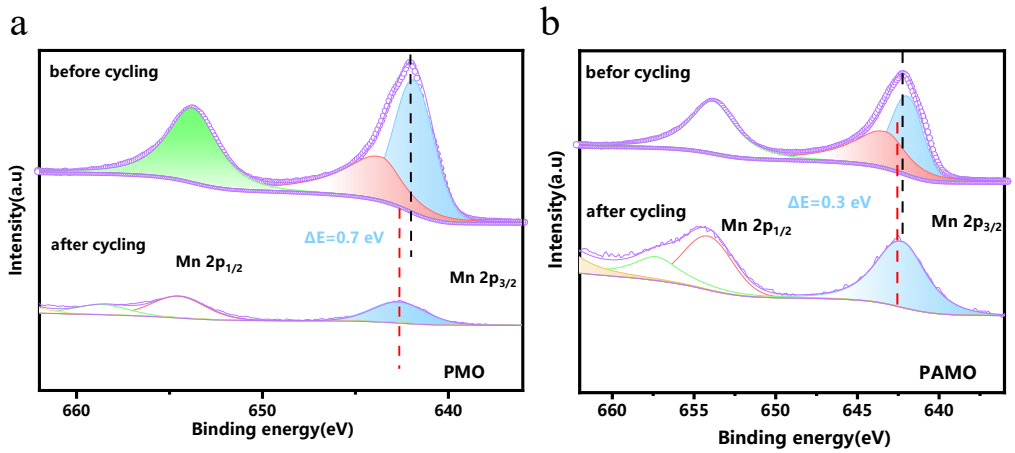

Figure S8. X-ray photoelectron spectroscopy (XPS) of zinc-manganese batteries prepared with (a) PMO and (b) PAMO as cathode materials after charge-discharge cycles at a current density of 1 A g^{-1}.

Table S1. Statisical table of O content of PAMO and PMO.

Modified sample	Lattice O	O_v	Hydroxyl species
PAMO	**56.06%**	**21.23%**	**22.71%**
PMO	**54.79%**	**12.9%**	**32.31%**

Table S2. Electrochemical parameters fitted by electrochemical impedance spectroscopy of all samples.

Samples	Rct / Ω	Rs / Ω
PAMO	**7.83**	**2.12**
PMO	**7.92**	**2.61**
MO	**8.31**	**4.53**